Relations of Progression in Cognitive Decline with Initial EEG Resting-State Functional Network in Mild Cognitive Impairment

Chia-Feng Lu, Yuh-Jen Wang, Yu-Te Wu, Sui-Hing Yan

Abstract—This study aimed at investigating whether the functional brain networks constructed using the initial EEG (obtained when patients first visited hospital) can be correlated with the progression of cognitive decline calculated as the changes of mini-mental state examination (MMSE) scores between the latest and initial examinations. We integrated the time–frequency cross mutual information (TFCMI) method to estimate the EEG functional connectivity between cortical regions, and the network analysis based on graph theory to investigate the organization of functional networks in aMCI. Our finding suggested that higher integrated functional network with sufficient connection strengths, dense connection between local regions, and high network efficiency in processing information at the initial stage may result in a better prognosis of the subsequent cognitive functions for aMCI. In conclusion, the functional connectivity can be a useful biomarker to assist in prediction of cognitive declines in aMCI.

Keywords—Cognitive decline, functional connectivity, MCI, MMSE.

I. INTRODUCTION

MILD cognitive impairment (MCI) was regarded as an intermediate state of cognitive function between changes seen in normal aging and those fulfilling the criteria for Alzheimer's disease (AD) [1]. MCI, especially the amnestic subtype MCI (aMCI), may convert to AD at about 30-50% within 3-5 years, which is much more higher than the conversion rate in normal aging individuals [2]-[4]. Accordingly, identifying a neurophysiological marker that is associated with the progression of cognitive decline in aMCI is of clinical importance.

Previous studies reported that aMCI were not only associated with regional alterations, but also with disrupted functional integration between different brain regions, and therefore aMCI were considered as a disconnection syndrome

C. F. Lu and Y. J. Wang contributed equally to this article.
C. F. Lu is with the Image Research Center, College of Medicine, Taipei Medical University, Taipei, Taiwan; Department of Physical Therapy and Assistive Technology, National Yang-Ming University, Taipei, Taiwan; and with the Department of Education and Research, Taipei City Hospital, Taipei, Taiwan (e-mail: alvin4016@yahoo.com.tw).
Y. J. Wang is with the Department of Neurology, Taipei City Hospital, Ren-Ai Branch, Taipei, Taiwan (e-mail: DAL29@tpech.gov.tw).
Y. T. Wu is with the Institute of Biophotonics, National Yang-Ming University, Taipei, Taiwan (e-mail:ytwu@ym.edu.tw).
S. H. Yan is with the Department of Neurology, Taipei City Hospital, Ren-Ai Branch, Taipei, Taiwan (corresponding author, phone: +886-2-2709-3600 ext.3711; fax: +886-2-2704-6356; e-mail: DAK02@tpech.gov.tw).

[5]. To investigate the network architecture in aMCI, we used functional connectivity analysis based on the resting-state electroencephography (EEG) data for 21 patients with aMCI and further correlated the properties of functional networks with the changes of cognitive functions.

Functional connectivity can be measured by estimating synchrony of the EEG signal oscillations between cortical regions. The conventional coherence analysis was commonly used to measure functional connections; however, it only measures linear dependency between neural signals and may be insufficient for studying complex and nonlinear brain dynamics [6]. Furthermore, the coherence method can be problematic if the signals are contaminated by noise or the oscillatory frequency band is not carefully defined [7], [8]. The time–frequency cross mutual information (TFCMI) method offers an alternative solution [9], [10], which calculates the mutual information between two temporal power sequences within a specific band, and serves as a statistical measure of linear and nonlinear dependencies between cortical regions [11].

In the present study, we integrated the TFCMI method to estimate the EEG functional connectivity between cortical regions followed by the network analysis based on graph theory to investigate the network organization for six different frequency bands, including delta, theta, alpha, beta1, beta2, and gamma bands. This study aimed at investigating whether the functional brain networks constructed using the initial EEG (obtained when patients first visited Taipei City Hospital) can be correlated with the progression of cognitive decline calculated as the changes of mini-mental state examination (MMSE) scores between the latest and initial examinations. We hypothesized that the integrity of functional network at the initial stage, characterized by the strengths of functional connectivity, density of between locally functional-connected regions, and network efficiency in information transmission, may be a useful biomarker to predict the subsequent declines in cognitive functions for aMCI.

II. MATERIALS AND METHODS

A. Participants

This study received prior approval from the Institutional Review Board of Taipei City Hospital. We retrospectively enrolled amnestic subtype of MCI (aMCI) patients with EEG examinations. Their clinical data regarding dementia and cognitive decline were collected, including clinical histories,

neurological examinations, neuroimaging studies (CT or MRI), neuropsychological interview, mini-mental state examination (MMSE) [12], and clinical dementia rating (CDR) [13], when they first visited the Department of Neurology in Taipei City Hospital during 2008-2011. All recorded clinical data were reviewed by two expert neurologists (Y.J. Wang and S.H. Yan) to exclude participants with (1) evidence of other neurological or psychiatric diseases characterized by the cognitive impairment; (2) uncontrolled or complicated systemic diseases or traumatic brain injuries.

The diagnosis of aMCI met the Petersen criteria [4]. The inclusion criteria for aMCI participants in this study were: (1) CDR score of 0.5; (2) MMSE score of 20–25; and (3) memory decline in the absence of dementia or significant functional loss. Finally, the clinical data and EEG of 21 aMCI (5 males and 16 females) were enrolled in this study for the subsequent analysis.

The 1-year and the latest follow-up MMSE after the first EEG examination for aMCI patients were also collected in this study. The 1-year and the latest follow-up MMSE were separately compared with the initial MMSE to determine whether the follow-up MMSE were significant different from the initial MMSE using paired t test. Only the latest MMSE were significantly decreased ($p = 0.022$) compared with the initial MMSE. Table I summarizes the demographic features and clinical data of aMCI patients.

TABLE I
DEMOGRAPHIC FEATURES AND CLINICAL DATA OF aMCI

No.	Sex	Age	Initial MMSE	1-year MMSE	Latest MMSE	Initial-to-latest duration (months)
1	M	86	26	--	23	48
2	M	81	21	21	20	50
3	M	84	26	--	19	52
4	F	87	21	24	25	26
5	F	82	25	23	23	15
6	F	78	12	--	14	45
7	M	85	23	25	14	24
8	F	83	18	16	21	19
9	F	83	9	15	14	53
10	F	81	22	21	14	48
11	F	82	22	20	21	34
12	F	70	20	23	21	40
13	F	75	22	20	20	13
14	F	79	26	19	22	31
15	F	82	13	--	10	34
16	F	76	13	14	10	38
17	F	79	21	21	22	53
18	F	84	25	25	24	62
19	F	84	17	19	9	52
20	F	80	24	20	17	34
21	M	82	25	26	22	44
p value	--	--	--	0.442	0.022	--
mean	--	81.1 ± 4.0	20.5 ± 5.1	20.7 ± 3.5	18.3 ± 5.0	38.8 ± 13.8

MMSE, mini-mental state examination.

B. EEG Recordings and Preprocessing

The EEG data during resting state were recorded from 19 scalp electrodes using a Nihon-Kohden EEG-1000 system (Nihon-Kohden Inc., Tokyo, Japan) at a sampling rate of 200 Hz and impedance of less than 7 kΩ at each electrode. The 19 electrodes were positioned according to the international 10–20 system including Fp1, Fp2, F3, F4, C3, C4, P3, P4, O1, O2, F7, F8, T3, T4, T5, T6, Fz, Cz, and Pz. All the EEG activities were referenced to the average signal of the two linked mastoid electrodes and bandpass filtered between 1 and 40 Hz. Both eyes-closed and eyes-opened conditions were recorded for 20–30 s alternately to a total of 4 minutes for each condition. Subjects remained awake and alert during the recording without increased attentional demand or cognitive load. Only the eyes-closed EEG data were extracted and segmented into approximate 110 consecutive epochs of 2 s in the present study.

To eliminate the ocular, muscular, and other types of physiological artifacts, we first reviewed each epoch and manually discarded the bad epochs with aberrant waveforms or large signal drifts. The averaged rejection rates of epochs are $24.90 \pm 9.94\%$. Second, the algorithm of independent component analysis was utilized to decompose the EEG signals into multiple independent components, allowing artifacts to be easily detected and rejected [14]. The rejection criteria of independent components were that: (1) the scalp voltage map presents a far-frontal projection which is a typical artifact of eye movement; (2) the map is marginally localized with high-frequency powers; or (3) the component activities originated from few specific epochs and did not consistently distribute across epochs. The number of rejected components is $3.38 \pm 1.69\%$. Finally, approximate 80 artifact-free epochs for each participant were used for further analysis.

C. Source Signal Estimation

In this study, the signals of cortical source were estimated from the scalp EEG data by two steps, namely, the forward model followed by an inverse operation. The forward head model was constructed based on a symmetric boundary element using OpenMEEG package (http://openmeeg.github.io/) [15]. To compute the inverse operator, minimum-norm estimation (MNE) with depth-weighting approach was used to obtain the source signals along the entire cortical surface of the EEG data [16]. The specific parameters are given as follows: (a) the source orientations were set to be unconstrained on the cortical surface; (b) a depth weighting algorithm was used to compensate for the biased calculations of superficial sources [17]; and (c) a regularization parameter, $\lambda^2 = 0.1$, was used to reduce numerical instability of the MNE and obtain a spatially smoothed solution [16]. The MNE analysis was performed using Brainstorm software (http://neuroimage.usc.edu/brainstorm) [18].

Cortical surface maps of source activity in each subject were displayed on the standard Colin27 anatomical images in Montreal Neurological Institute (MNI) space [19]. We further extracted the time-varying current strengths in 62 cortical surface regions covering entire cerebral cortex for each epoch based on a Mindboggle atlas (Table II) [20].

TABLE II
CORTICAL SURFACE REGIONS AND THEIR ABBREVIATIONS
(ALL FOR BOTH HEMISPHERES)

Type	Name	Label	Type	Name	Label
PF	Medial orbitofrontal	MOF	PF	Lateral orbitofrontal	LOF
PF	Parsorbitalis	PO	F	Superior frontal	SF
F	Caudal middle frontal	CMF	F	Rostral middle frontal	RMF
F	Parsopercularis	POP	F	Parstrangularis	PT
C	Paracentral	paraC	C	Precentral	preC
C	Postcentral	postC	P	Precuneus	precun
P	Surperior parietal	SP	P	Inferior parietal	IP
P	Supramarginal	SM	T	Superior temporal	ST
T	Middle temporal	MT	T	Inferior temporal	IT
T	Transverse temporal	TT	T	Insula	insula
T	Parahippocampus	paraH	T	Entrohinal	EC
T	Fusiform	fusiform	L	Rostral anterior cingulate	RAC
L	Caudal anterior cingulate	CAC	L	Posterior cingulate	PC
L	Isthmus cingulate	IC	O	Cuneus	cuneus
O	Lingual	lingual	O	Pericalcarine	periCal
O	Lateral occipital	LO			

PF, prefrontal; F, frontal; C, central; P, parietal; T, temporal; L, limbic; O, occipital.

D. Brain Network Construction

The functional brain network for each participant was represented by a 62×62 graph consisting of 62 nodes (cortical regions) and edges (functional connectivity between regions). The functional connectivity between cortical surface regions was measured using the time-frequency cross mutual information (TFCMI) analysis, which is more resistant to reference selection and noise interference than the coherence method [9], [10]. The TFCMI analysis consists of two processing steps, i.e. the wavelet transformation and mutual information calculation. First, the surface source signal in each region and each epoch was transformed into the time-frequency domain using the Morlet wavelet transformation to obtain temporal spectral map (Fig. 1 (b)) [9]. The frequency resolution was 1 Hz and temporal resolution was 5 ms. Six sets of time-frequency maps encompassing the *delta* (1-4 Hz), *theta* (5-7 Hz), *alpha* (8-12 Hz), *beta1* (13-20 Hz), *beta2* (21-30 Hz), and *gamma* (31-40 Hz) activities were created separately. The power across selected frequency bands in each cortical region was averaged to produce a dynamic power curve (Fig. 1 (c)). The temporal series of averaged power signals were then used to compute the cross mutual information (CMI) between any two cortical regions in each epoch [9]. Denote the averaged power signals at the *i*th region by a random variable, F_i, and its probability density function (PDF) by $p(F_i)$.

$$CMI_{i,j} = \sum_{b=1}^{40} p(F_{i,b}, F_{j,b}) \ln\left(p(F_{i,b}, F_{j,b}) / p(F_{i,b}) p(F_{j,b}) \right), \quad (1)$$

where b=1,2,…,40 represents the index of sampling bins used to construct the approximated PDF and joint PDF. Finally, the functional connections in each epoch and each frequency band were generated by a pair of regions, creating a 62×62 TFCMI

map (Fig. 1 (d)). The TFCMI values were normalized so that the maximal values equal one. A schematic diagram for the construction of a functional network is shown in Fig. 1.
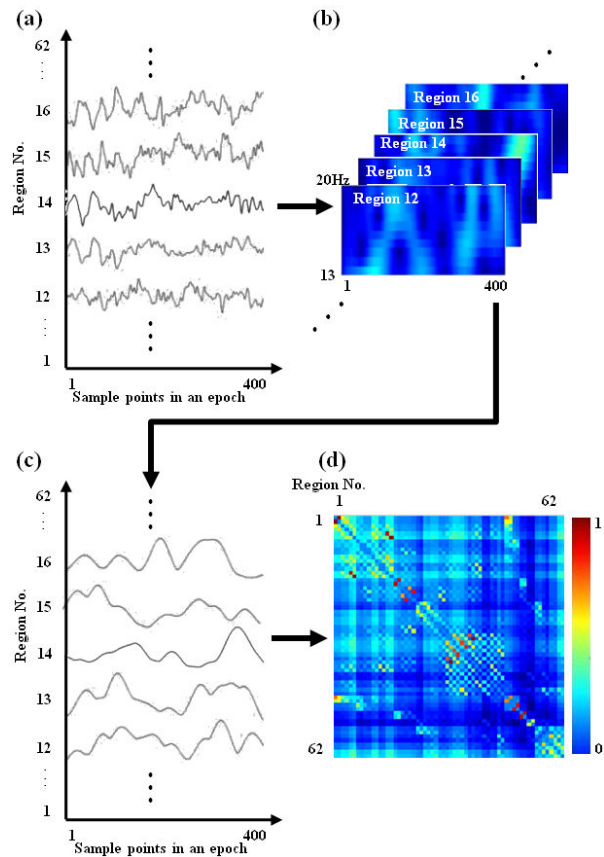

Fig. 1 Schematic diagram of the functional network construction (a) The EEG source signals for 62 cortical surface regions of each epoch. (b) The source signal were processed using the Morlet wavelet transformation to obtain time–frequency power maps within the selected frequency band (beta1, 13–20 Hz shown here), in which colors indicate power amplitude in an arbitrary unit (a. u.). (c) The averaged power signal for each region was created by averaging the individual time–frequency maps across selected frequency band. (d) The 62×62 TFCMI map was obtained by calculating the cross mutual information from the averaged powers between any two channels

E. Network Analysis

The 62×62 TFCMI maps for each selected frequency band were first binarized by applying threshold T to the weighted edges.

$$e_{ij} = \begin{cases} 1, & \text{if } CMI_{i,j} \geq T \\ 0, & \text{otherwise} \end{cases} \quad (2)$$

where e_{ij} is referred to as the effective connection between cortical regions *i* and *j*. We set thresholds T equal to the mean value of whole TFCMI map added by one standard deviation for all participants. The threshold for each selected band in this study was 0.53 in delta, 0.42 in theta, 0.35 in alpha, 0.29 in beta1, 0.23 in beta2, and 0.19 in gamma, respectively.

Network organization can be estimated by topological properties based on graph theory. Two regional properties, including nodal clustering coefficient (C_i) and nodal shortest path length (L_i) were computed for each node. The nodal clustering coefficient is the probability of interconnectivity between neighboring nodes in a network; the nodal shortest path length represents the separation between any pair of nodes in a network [21]-[24]. The topological properties were calculated as follows:

$$k_i = \sum_{j \in N} e_{ij} \tag{3}$$

$$C_i = (1/k_i(k_i - 1)) \sum_{j,h \in N} e_{ij} e_{ih} e_{jh} \tag{4}$$

$$L_i = \frac{1}{n-1} \sum_{j \in N, j \neq i} d_{ij} \tag{5}$$

where k_i is the number of functionally connected neighbors to the node i, n is the number of nodes, N is the set of full brain network, and d_{ij} is the minimal number of edges that must be traversed to form a connection between nodes i and j.

F. Statistics

Since only the latest MMSE for the recruited aMCI patient were significantly different (p < 0.05 using paired t test) from the initial MMSE (Table I), we calculated the changes in MMSE as the difference between the latest and initial MMSE and denoted it as ΔMMSE (= MMSE_latest - MMSE_initial). Therefore, a negative value of ΔMMSE represents the cognitive decline for a patient.

We examined the relationships between the strength of each functional connectivity and ΔMMSE for aMCI patients using partial correlation coefficients controlling for age, sex, and initial-to-latest duration as confounding variables to confirm that the correlation analysis would not be biased by the various initial-to-latest durations across patients. The significant correlations were identified as $p < 0.05$ with false discovery rate (FDR) method for multiple comparisons [25]. Similarly, the relationships between the ΔMMSE and two topological properties (C_i and L_i) for each cortical region (node) were calculated using partial correlation coefficients controlling for potential confounding variables.

III. RESULTS AND DISCUSSIONS

A. Functional Connectivity and Changes in MMSE

The significant correlations between the strength of functional connectivity and ΔMMSE in different frequency bands are displayed in Fig. 2. All the significant correlations were positive correlations suggesting that stronger functional connectivity between cortical regions calculated from the initial EEG data may indicate larger values (less negative or more positive) of ΔMMSE, namely, less reduction in the subsequent MMSE. The results showed that more significantly positive correlations and more symmetric patterns across left and right

hemispheres can be found in higher frequency bands compared with the findings in lower frequency bands (Fig. 2). Most functional connectivity with significant correlations with ΔMMSE were the "long-distance" connections referring to the functional connectivity between distant brain regions, such as frontal-parietal, frontal-occipital, and frontal-temporal connections. Our results were in line with the previous reports that the progressive aMCI or AD usually exhibited the disruptions of long distance connectivity, especially related to the frontal cortex and anterior limbic systems [26]-[28]. The left lateralization of functional connectivity with significant correlations with ΔMMSE was found in the lower frequency bands (Figs. 2 (a)-(d)).

Moreover, the core regions that had the most functional connections with other regions exhibiting significant correlations with ΔMMSE were located at the medial and lateral orbitofrontal regions (LOF and MOF) and rostral anterior cingulate (RAC).
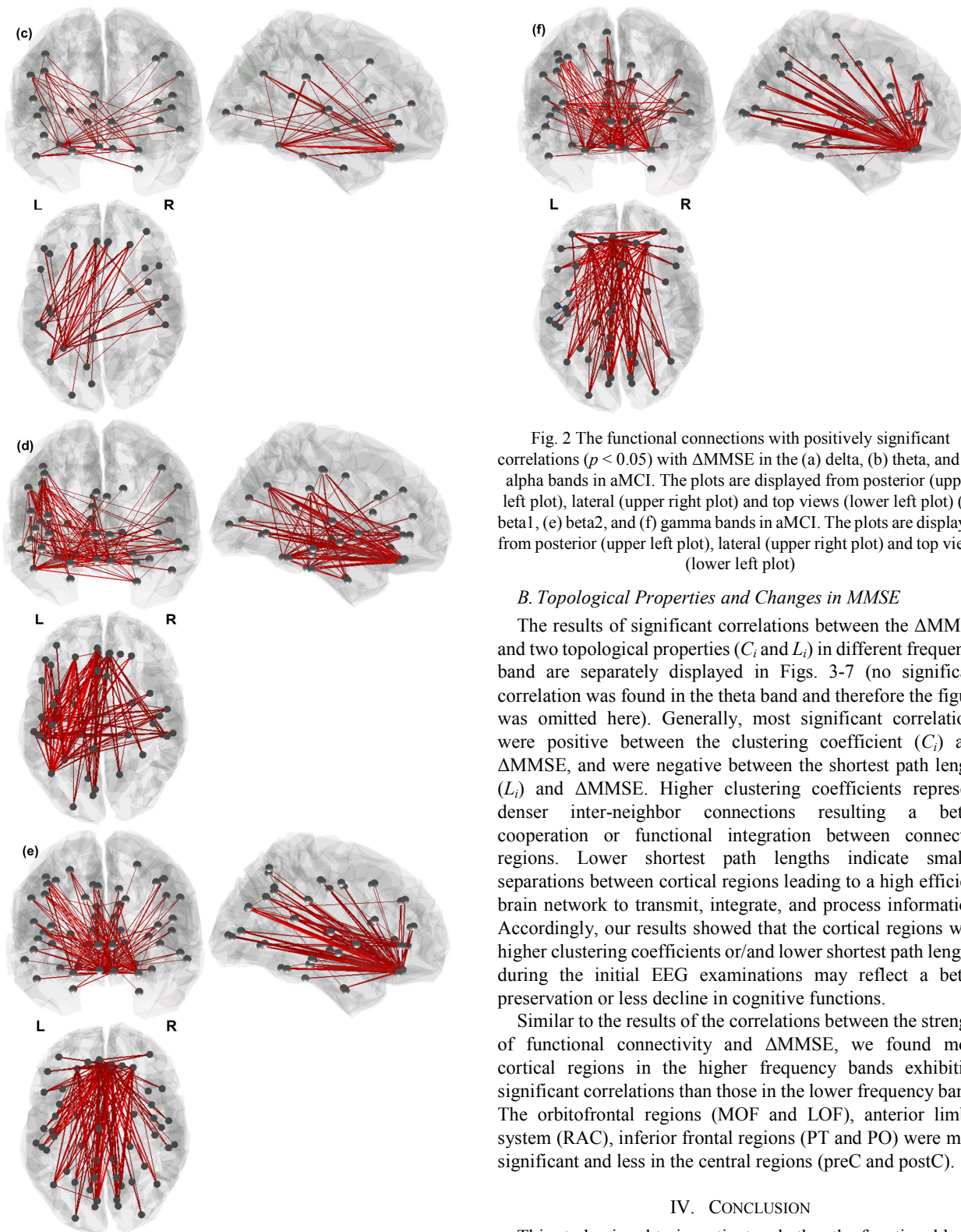

(a)

L   R

(b)

L   R
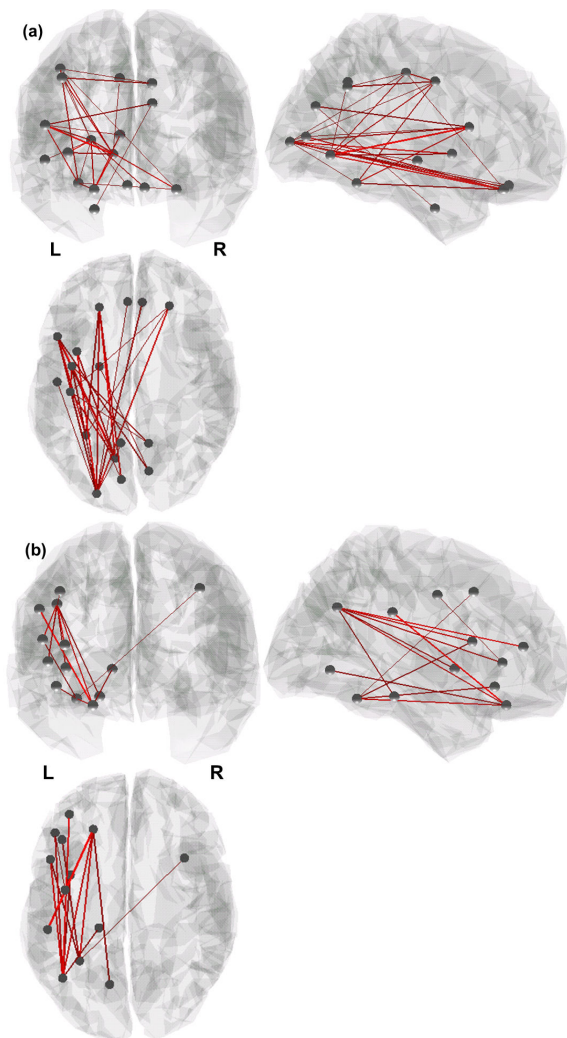
Fig. 2 The functional connections with positively significant correlations ($p < 0.05$) with ΔMMSE in the (a) delta, (b) theta, and (c) alpha bands in aMCI. The plots are displayed from posterior (upper left plot), lateral (upper right plot) and top views (lower left plot) (d) beta1, (e) beta2, and (f) gamma bands in aMCI. The plots are displayed from posterior (upper left plot), lateral (upper right plot) and top views (lower left plot)

B. Topological Properties and Changes in MMSE

The results of significant correlations between the ΔMMSE and two topological properties (C_i and L_i) in different frequency band are separately displayed in Figs. 3-7 (no significant correlation was found in the theta band and therefore the figure was omitted here). Generally, most significant correlations were positive between the clustering coefficient (C_i) and ΔMMSE, and were negative between the shortest path length (L_i) and ΔMMSE. Higher clustering coefficients represent denser inter-neighbor connections resulting a better cooperation or functional integration between connected regions. Lower shortest path lengths indicate smaller separations between cortical regions leading to a high efficient brain network to transmit, integrate, and process information. Accordingly, our results showed that the cortical regions with higher clustering coefficients or/and lower shortest path lengths during the initial EEG examinations may reflect a better preservation or less decline in cognitive functions.

Similar to the results of the correlations between the strength of functional connectivity and ΔMMSE, we found more cortical regions in the higher frequency bands exhibiting significant correlations than those in the lower frequency bands. The orbitofrontal regions (MOF and LOF), anterior limbic system (RAC), inferior frontal regions (PT and PO) were most significant and less in the central regions (preC and postC).

IV. CONCLUSION

This study aimed to investigate whether the functional brain networks constructed using the initial EEG were correlated with the changes in cognitive decline (ΔMMSE) between the latest and initial examinations. Our findings in local connection

strengths and nodal topological properties were in line with the previous literatures. The results supported our hypothesis that higher integrated functional network with sufficient connection strengths, dense connection between local regions, and high network efficiency in processing information at the initial stage can be a basis to anticipate better prognosis of the subsequent cognitive functions for aMCI.
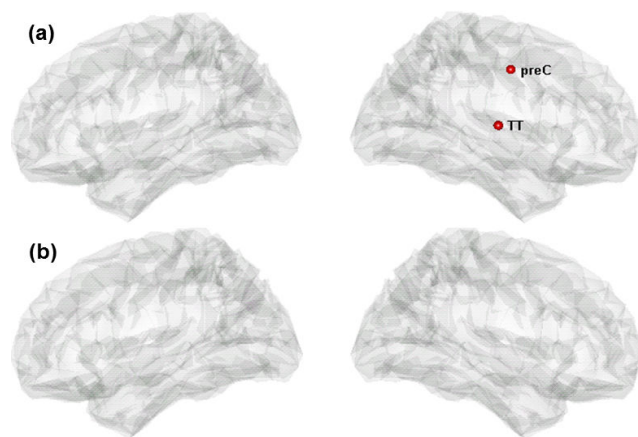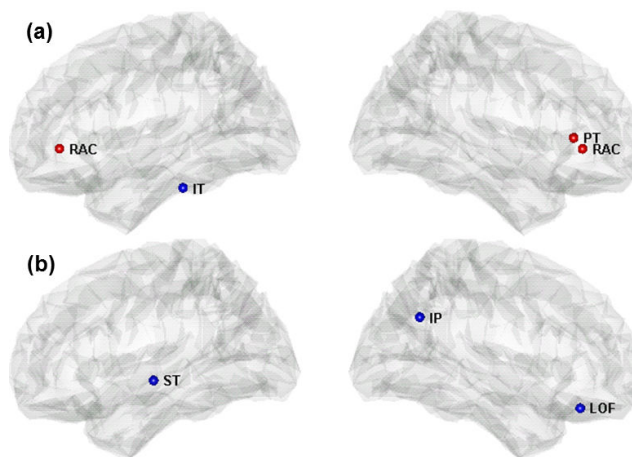

Fig. 3 The cortical regions with significant correlations (red for positive and blue for negative) between (a) the clustering coefficient and ΔMMSE; and (b) the shortest path length and ΔMMSE in the *delta* band. The plots are displayed from left (left column) and right (right column) lateral views
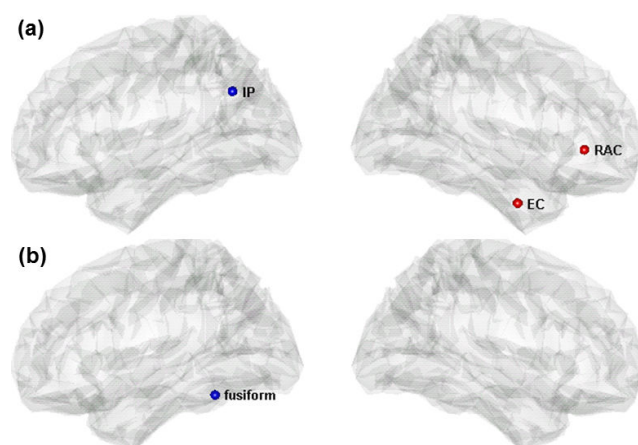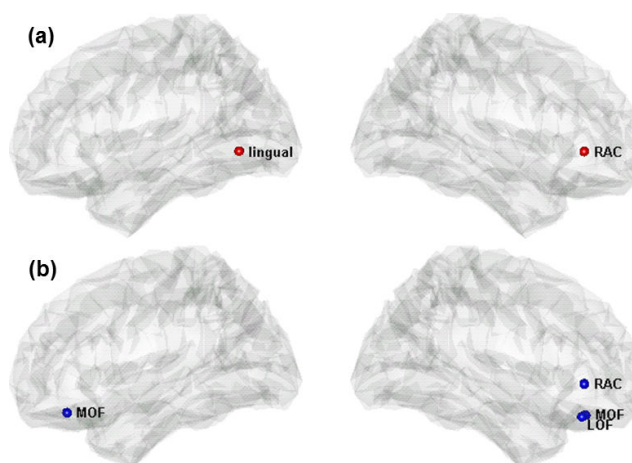

Fig. 4 The cortical regions with significant correlations (red for positive and blue for negative) between (a) the clustering coefficient and ΔMMSE; and (b) the shortest path length and ΔMMSE in the *alpha* band. The plots are displayed from left (left column) and right (right column) lateral views

Fig. 5 The cortical regions with significant correlations (red for positive and blue for negative) between (a) the clustering coefficient and ΔMMSE; and (b) the shortest path length and ΔMMSE in the *beta1* band. The plots are displayed from left (left column) and right (right column) lateral views
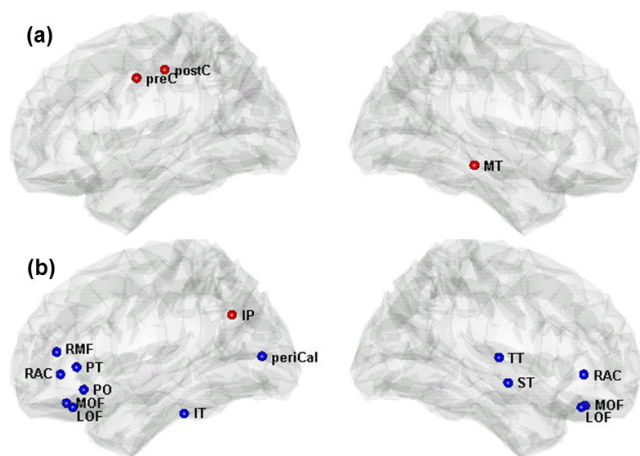

Fig. 6 The cortical regions with significant correlations (red for positive and blue for negative) between (a) the clustering coefficient and ΔMMSE; and (b) the shortest path length and ΔMMSE in the *beta2* band. The plots are displayed from left (left column) and right (right column) lateral views

Fig. 7 The cortical regions with significant correlations (red for positive and blue for negative) between (a) the clustering coefficient and ΔMMSE; and (b) the shortest path length and ΔMMSE in the *gamma* band. The plots are displayed from left (left column) and right (right column) lateral views

REFERENCES

[1] R. C. Petersen, "Early diagnosis of Alzheimer's disease: is MCI too late?," *Current Alzheimer Research*, vol. 6, p. 324, 2009.
[2] A. Pozueta, E. Rodríguez-Rodríguez, J. L. Vazquez-Higuera, I. Mateo, P. Sánchez-Juan, S. González-Perez, J. Berciano, and O. Combarros, "Detection of early Alzheimer's disease in MCI patients by the combination of MMSE and an episodic memory test," *BMC neurology*, vol. 11, p. 78, 2011.
[3] S. Landau, D. Harvey, C. Madison, E. Reiman, N. Foster, P. Aisen, R. Petersen, L. Shaw, J. Trojanowski, and C. Jack, "Comparing predictors of conversion and decline in mild cognitive impairment," *Neurology*, vol. 75, pp. 230-238, 2010.
[4] R.C. Petersen, "Mild cognitive impairment as a diagnostic entity," *J. Intern. Med.*, vol. 256, pp. 183–194, 2004.
[5] P. Missonnier, M. P. Deiber, G. Gold, F.R. Herrmann, P. Millet, A. Michon, L. Fazio-Costa, V. Ibañez, P. Giannakopoulos, "Working memory load–related electroencephalographic parameters can differentiate progressive from stable mild cognitive impairment," *Neuroscience*, vol. 150, Issue 2, pp. 346-356, 2007.
[6] D. Popivanov, J. Dushanova, "Non-linear EEG dynamic changes and their probable relation to voluntary movement organization," *Neuroreport*, vol. 10, pp. 1397–401, 1999.
[7] C. Andrew, G. Pfurtscheller, "Lack of bilateral coherence of post-movement central beta oscillations in the human electroencephalogram," *Neurosci. Lett.*, vol. 273, pp. 89–92, 1999.
[8] P.L. Nunez, R. Srinivasan, A.F. Westdorp, R.S. Wijesinghe, D.M. Tucker, R.B. Silberstein et al., "EEG coherency: I: statistics, reference electrode, volume conduction, Laplacians, cortical imaging, and interpretation at multiple scales," *Electroencephalogr. Clin . Neurophysiol.*, vol. 103, pp. 499–515, 1997.
[9] C.F. Lu, S. Teng, C.I. Hung, P.J. Tseng, L.T. Lin, P.L. Lee, Y.T. Wu, "Reorganization of functional connectivity during the motor task using EEG time–frequency cross mutual information analysis," *Clinical Neurophysiology*, vol. 122, no. 8, pp. 1569-1579, 2011.
[10] C.C. Chen, J.C. Hsieh, Y.Z. Wu, P.L. Lee, S.S. Chen, D.M. Niddam, T.C. Yeh, Y.T. Wu, "Mutual-information-based approach for neural connectivity during self-paced finger lifting task," *Human brain mapping*, vol. 29, no. 3, pp. 265-280, 2008.
[11] C. Shannon, "A mathematical theory of communication," *Bell Syst Tech J*, vol. 27, pp. 379–426, 1948.
[12] M.F. Folstein, S.E. Folstein, P.R. McHugh, "Mini-mental state. A practical method for grading the cognitive state of patients for the clinician," *J. Psychiatr. Res.*, vol. 12, pp. 189–198, 1975.
[13] J.C. Morris, "The Clinical Dementia Rating (CDR): current version and scoring rules," *Neurology*, vol. 43, pp. 2412–2414, 1993.
[14] A. Delorme, S. Makeig, "EEGLAB: an open source toolbox for analysis of single-trial EEG dynamics including independent component analysis." *J. Neurosci. Methods.*, vol. 134, pp. 9–21, 2004.
[15] A. Gramfort, T. Papadopoulo, E. Olivi, M. Clerc, "OpenMEEG: opensource software for quasistatic bioelectromagnetics," *BioMedical Engineering OnLine*, vol. 9, no. 1, pp.45, 2010.
[16] M.S. Hamalainen, R.J. Ilmoniemi, "Interpreting magnetic fields of the brain: minimum norm estimates," *Med. Biol. Eng. Comput.*, vol. 32, pp. 35–42, 1994.
[17] F.H. Lin, T. Witzel, S.P. Ahlfors, S.M. Stufflebeam, J.W. Belliveau et al, "Assessing and improving the spatial accuracy in MEG source localization by depth-weighted minimum-norm estimates," *Neuroimage*, vol. 31, pp. 160–171, 2006.
[18] F. Tadel, S. Baillet, J.C. Mosher, D. Pantazis, R.M. Leahy, "Brainstorm: a user-friendly application for MEG/EEG analysis," *Comput. Intell. Neurosci.*, 879716, 2011..
[19] D.L. Collins, A.P. Zijdenbos, V. Kollokian et al., "Design and construction of a realistic digital brain phantom," *IEEE Transactions on Medical Imaging*, vol. 17, no. 3, pp. 463–468, 1998.
[20] A. Klein, J. Tourville, "101 labeled brain images and a consistent human cortical labeling protocol," *Frontiers in neuroscience*, vol. 6, article 171, 2012.
[21] M.D. Humphries, K. Gurney, "Network 'Small-world-ness': a quantitative method for determining canonical network equivalence," *PLoS One*, vol. 3, article e0002051, 2008.
[22] V. Latora, M. Marchiori, "Efficient behavior of small-world networks," *Phys. Rev. Lett.*, vol. 87, article 198701, 2001.
[23] E. Bullmore, O. Sporns, "Complex brain networks: graph theoretical analysis of structural and functional systems," *Nat. Rev. Neurosci.*, vol. 10, pp. 186–198, 2009.
[24] S. Achard, E. Bullmore, "Efficiency and cost of economical brain functional networks," *PLoS Comput. Biol.*, vol. 3, no. 2, article e17, 2007.
[25] Y. Benjamini, Y. Hochberg, "Controlling the false discovery rate: a practical and powerful approach to multiple testing," *J. R. Stat. Soc. Series B Stat. Methodol.*, vol. 57, pp. 289–300, 1995.
[26] Y. He, Z. Chen, G. Gong, A. Evans, "Neuronal Networks in Alzheimer's Disease," *Neuroscientist*, vol. 15, pp. 333-350, 2009.
[27] Y. Liu, C. Yu, X. Zhang, J. Liu, Y. Duan, A.F. Alexander-Bloch, B. Liu, T. Jiang, E. Bullmore, "Impaired long distance functional connectivity and weighted network architecture in Alzheimer's disease," *Cerebral Cortex*, vol. 24, no. 6, pp.1422-1435, 2014.
[28] B. Tóth, B. File, R. Boha, Z. Kardos, Z. Hidasi, Z.A. Gaál, E. Csibri, P. Salacz, C.J. Stam, M. Molnár, "EEG network connectivity changes in mild cognitive impairment — Preliminary results," *International Journal of Psychophysiology*, vol. 92, Issue 1, pp. 1-7, 2014.